

Testing Performance of Low Voltage Arresters

Waluyo and Yan Maret Hutasoit

Department of Electrical Engineering, National Institute of Technology (Itenas) Bandung 40124, Indonesia

Received: March 24, 2016 / Accepted: April 05, 2016 / Published: June 30, 2016.

Abstract: Due to important consideration of protection against lightning surge on electrical, electronic and telecommunication equipment, it was necessary to carry out a special study to look at the performance of protective devices. The study was testing performance of arresters on low voltage system. The activity was testing of arresters using steady state and impulse voltages. The arresters consisted of gas tube, zener diode, varistor and spark gap arresters, then it was made a cascade circuit between the varistor and spark gap arresters with a decoupling element. The decoupling elements were used air, iron and ferrite. The test yielded data of current and voltage on the tables and oscilloscope waveforms. The arresters had cut voltages early different from each other, namely the gas tube, zener diode, spark gap and varistor arresters were at the voltages of 500 V, 250 V, 1,000 V and 565 V respectively. The iron core decoupling element cascade circuit had the least oscillation among remaining cores.

Key words: Arrester, cascade, decoupling element, gas tube, impulse, varistor, zener diode.

1. Introduction

Franklin performed his initial experiments on electricity. Lightning is a natural phenomenon with destructive consequences. When a lightning falls on a structure, its current generates an impulse surge. It needs arresters for lightning protection [1-5].

Lightning electromagnetic impulse radiation must be taken into consideration because they endanger electrical and electronic systems. In the case when no arrester was damaged or was not yet damaged by current in the flash, about 40% of the return stroke peak current and about 25% or more of the return stroke charge transferred in the first millisecond [6-7].

It has been studied urban cloud-to-ground lightning. It was found an average enhancement of 60-100% on the lightning activity over three large metropolitan areas. The CG-lightning activity was enhanced within and downwind of most of the urban areas. It has indicated that a significant enhancement of approximately 100% in negative and 50% in positive flash densities. The observed ball lightning was

produced from electric fields caused by the accumulation of ions [8-12].

Installation of arrester assures reliable lightning protection [13]. Due to integration with existing systems of substations, the developed device allows for reception of information regarding arrester discharges [14]. Switching transients are caused by energization and de-energization of system components [15]. The energy overloading criterion of the SPD (surge protective device) was considered in LV (low voltage) network [16].

Overvoltages generated by lightning discharges to overhead lines can cause flashover [17]. Choosing nice technology and higher capacity electronic components can make withstand capability higher [18]. The arresters are designed for using in category C locations, include on transformer secondary [19]. The unpredictable threat of transient overvoltage is ever increased in low voltage power supplies [20].

Gas discharge tubes have evolved to provide reliable and effective protection solutions during lightning storms and other electrical disturbances. The magnitudes and waveforms of the lightning overvoltages depend on many line and stroke

Corresponding author: Waluyo, research fields: electrical power transmission line and high voltage engineering.

parameters [21, 22]. The installation of lightning arresters helps decrease the adversarial effects resulting of lightning strike in the feeder [23]. Moisture and partial discharges can be present simultaneously and contribute to the varistor degradation. It is important to identify hot lightning arrester with an IP (internet protocol) camera [24, 25].

Lightning arresters must be able to discharge high-energy lightning currents. Surge arresters only serve limiting over voltages at relatively low-energy surge currents. Testing of surge arresters is very important [26, 27]. Using multiple spark gap arresters, it is even possible to not create any follow current [28].

Gas-filled surge arresters operate on gas-physical principle of highly effective arc discharge and very low leakage current. Earthing and bonding shall always be provided, directly or via suitable SPD. The arrester provides a low-impedance path to ground for current from a lightning strike or transient voltage and then restores to a normal operating condition. ZnO material has superiority over SiC. The important factors of arrester are environmental factors, electrical shocks, time of installing and number of operations. Surge current has become the standard parameter for comparing suppression devices. A varistor is used to limit voltage at terminals. A zener diode is equipped with a special structure to optimize its limiting behavior on transient surges [29-35].

The parameters adjustment of simplified IEEE (Institute of Electrical and Electronics Engineers) model was achieved for an MOSA (metal oxide surge arrester). The impulse current generator needs to be improved in reducing its overall inductance for ZnO surge arresters [36, 37]. Assessing condition of MOSA indicated a comparable degree of degradation [38]. SPDs are spark gaps, gas discharge tubes and metal oxide varistors. Electrical stresses can be power frequency, temporary over voltages, and impulse stresses resulting from switching and lightning [39, 40].

SPDs are tested differently. It is of great importance to understand the characteristics and the intended use of devices. The application of SPDs can reduce the local over voltages to acceptable limits. Surge arresters are to ensure appropriate insulation coordination and to protect valuable equipment from lightning and switching over voltages [41-44].

It is shown that the lightning strokes and their effects are very dangerous to electronics devices. Thus, the arrester role is significantly important. Practically on sites, the low voltage arresters are used to protect electrical devices that installed on power outlets, BNC (bayonet neill-concelman) probes, and various electronic equipment, telecommunication and information networks. Therefore, it is necessary to investigate the performance of low voltage arresters. The objective of research was investigating the performance of low voltage arresters by using the tests. The arrester kinds were gas tubes, varistors, zener diodes, spark gap arresters. The tests were both steady state and impulse conditions.

2. Testing Methods

The hybrid generator showed the peak voltage and peak current impulses, and they were also indicated on the oscilloscopes. The test equipment and arrester components are shown in Fig. 1.

The specifications of hybrid generator were 1-10 kV of oc voltage (1.2/50 μ s), 3 kA (max) of sc current (8/20 μ s) and 2 Ω of impedance. The specifications of spark gap arrester were 350 V/50 Hz of rated voltage (U_c), 75 kA of impulse current, I_{imp} (10/350 μ s), \leq

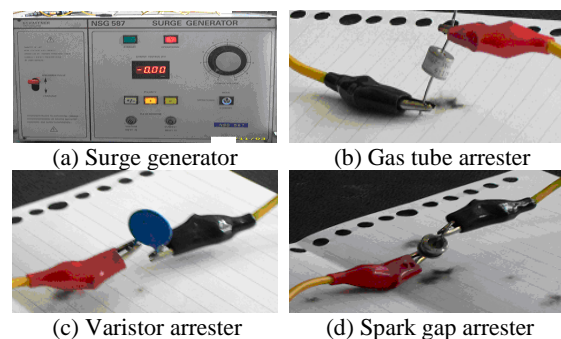


Fig. 1 Test equipment and arrester test objects.

1 kV of voltage protection level (1.2/50 μ s) and ≤ 100 ns of response time (t_A). The specifications of varistor were 100 V of U_c , 20 kA of nominal discharge current (I_{sn}), ≤ 1 kV at 5 kA (8/20 μ s) and ≤ 1.5 kV at I_{sn} of protection level voltage (U_p) and ≤ 25 ns of t_A . The specifications of gas tube arrester were 350 V/50 Hz of U_c , 70 kA of impulse current (10/350 μ s), I_{imp} , and ≤ 1 kV of U_p (1.2/50 μ s). The specifications of zener diode were 115 V of U_c and 10 kA of I_{sn} . In addition, the used decoupling element was 0.8 mm of wire diameter, whereas the cores were iron, ferrite and air, with 97 mm long and 8 mm diameter.

Fig. 2 shows the testing circuit of steady state conditions. Fig. 3a shows the impulse testing circuit on each arrester, and Fig. 3b shows the impulse testing circuit on cascade arresters.

The testing of gas tube arrester was in the way connected with the impulse generator with a positive impulse voltage (kV order) and the other end connected to the ground. The oscilloscope probe was connected to a series divider on the impulse generator. The tests were the same way for remaining arresters. The data of peak quantities were indicated on the generator panel. The voltage and current waveforms were shown on the oscilloscope.

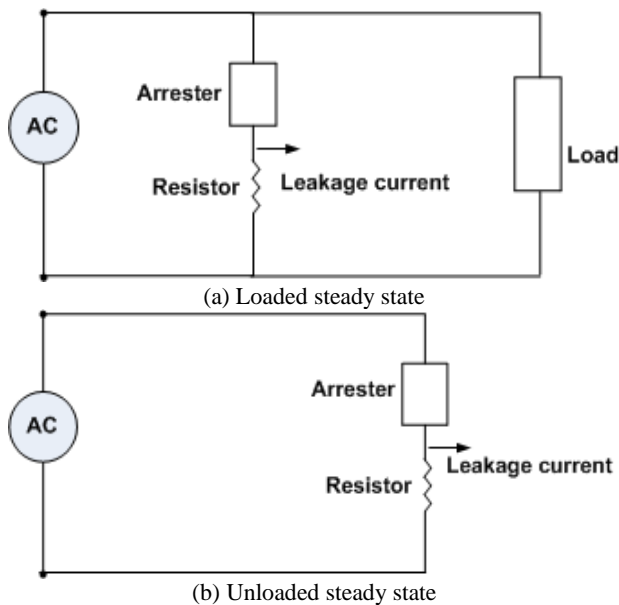


Fig. 2 Steady state testing circuits.

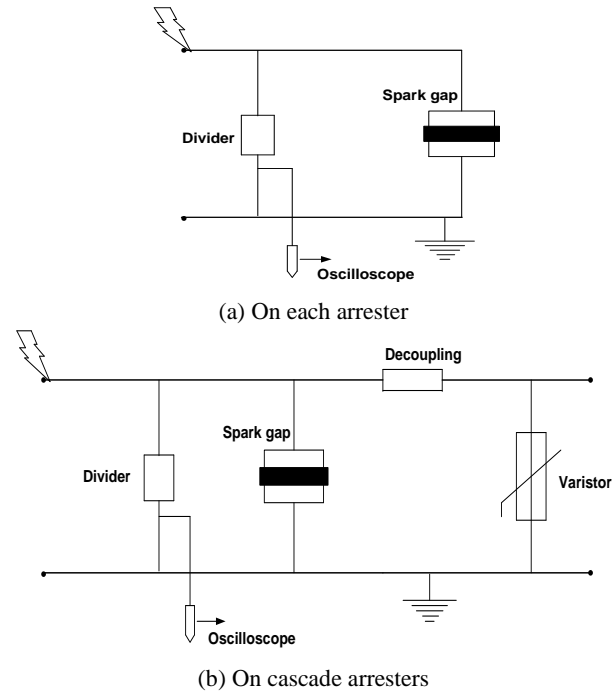


Fig. 3 Impulse testing circuits.

3. Test Results and Discussion

Table 1 lists the tests results of gas tube, zener diode, varistor and spark gap arresters, for steady state voltage without load, in range of 10 V to 200 V input voltages (V_i), peak-to-peak (V_{p-p}) and effective/rms voltages (V_{rms}).

Fig. 4 shows the curves of voltage values. The graph shows the slope tends to be constant, or does not get a change significantly. While, Table 2 lists the testing data of the arresters in steady state voltages with a load, in range of 10-200 V input voltages (V_i).

Table 1 No loading measurement result of arresters.

V_i (V)	Gas tube arrester (V)		Zener diode (V)		Varistor (V)		Spark gap arrester (V)	
	V_{p-p}	V_{rms}	V_{p-p}	V_{rms}	V_{p-p}	V_{rms}	V_{p-p}	V_{rms}
10	30	10.2	28	10	30	10.3	30	10.1
20	62	20.8	60	20.3	60	20.9	64	20.5
50	142	52.2	140	52.1	144	52.2	142	52.4
75	206	78.02	206	76.3	210	77.0	206	78.02
100	278	100	274	102	278	102	278	98.8
125	340	125	340	125	344	126	342	124
150	412	152	410	150	414	152	412	150
175	480	177	480	177	480	177	482	177
200	504	200	504	200	508	200	502	200

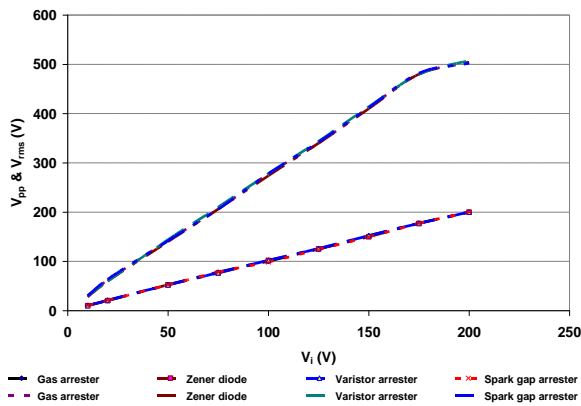
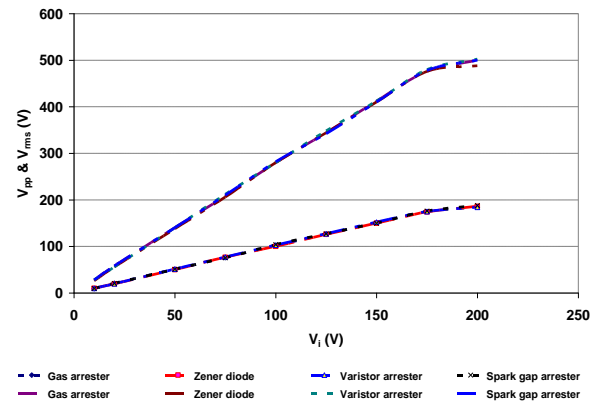
Fig. 4 Unloaded curves V_{pp} & V_{rms} - V_i testings.Fig. 5 Loaded curves of V_{pp} & V_r - V_p testings.

Table 2 Loaded measurement result of arresters.

V_i (V)	Gas tube arrester (V)		Zener diode (V)		Varistor (V)		Spark gap arrester (V)	
	V_{p-p}	V_{rms}	V_{p-p}	V_{rms}	V_{p-p}	V_{rms}	V_{p-p}	V_{rms}
10	28	9.4	26	10	28	10.2	28	9.5
20	58	20.7	56	19.6	56	19.8	58	20.6
50	140	51	138	50	140	51.2	140	51
75	208	75.8	206	76.5	212	76.9	210	75.6
100	280	102	280	100	280	103	282	104
125	344	126	344	126	348	127	342	127
150	412	151	410	150	412	152	410	150
175	476	175	476	174	480	175	478	176
200	500	184	488	186	502	184	500	188

From the curves in Fig. 5, the characteristics of the arrester were not much different from one another under normal circumstances either load or no-load. All arresters did not really give effect to the system, not interfere with voltage or current energy of supply. The leakage current or operating current of arresters was not visible from measurements using a multimeter or oscilloscope, and was not detected any voltage surge. On the high values of input voltages, the peak-to-peak voltages would be saturated. These cases were caused by the voltage drop due to the loading of circuits.

The testings of gas tube arrester with the impulses were done by subjecting range impulse voltage of 0.5-6 kV. The data were detected and recorded when the testing of gas tube arresters began to penetrate up to 6 kV of impulse voltage. The data are listed in Table 3.

The Table 3 lists impulse voltages (V_i), cut voltages (V_c) and cut currents (I_c), started the impulse voltage

Table 3 Measurement data of gas tube arrester.

V_i (V)	V_c (V)	I_c (A)
500	88	100
1,000	160	500
2,000	304	900
3,000	456	1,200
4,000	620	1,400
5,000	900	1,900
6,000	1,140	2,200

of 500 V with the cut voltage of 88 V and the cut current of 100 A. While, the samples of test waveforms are shown in Figs. 6 and 7.

Fig. 8 shows the V_c - V_i and I_c - V_i curves of the gas tube arrester. The cut voltage and current waveforms were almost constant. The voltage waveform was looked not directly towards zero, but there was little residue due to an arc voltage. The voltage and current waveforms show toward zero and go beyond the negative area. This case was caused the energy released by inductive components either in the arrester or generator circuit, where the currents were stored in the form of magnetic energy. The arrester absorbed energy would release in the form of thermal energy arc. Based on the figures, the measured cut impulse voltage and current waves were proportional to the input impulse voltages.

The testings of zener diode were done by applying the impulse voltages, from few hundreds of volts up to 1 kV, since above 1 kV, it would start to damage. This case was normal and it was quite dangerous to continue test above 1 kV. Table 4 lists the impulse voltage for

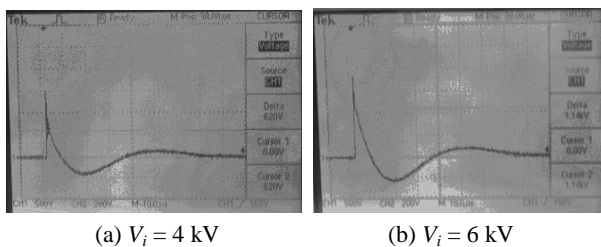


Fig. 6 Cut voltage waveforms of gas tube arrester.

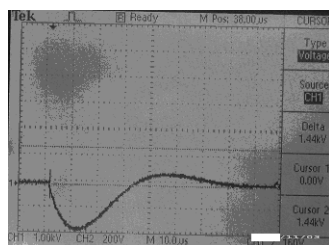


Fig. 7 Cut current waveform of gas tube arrester.

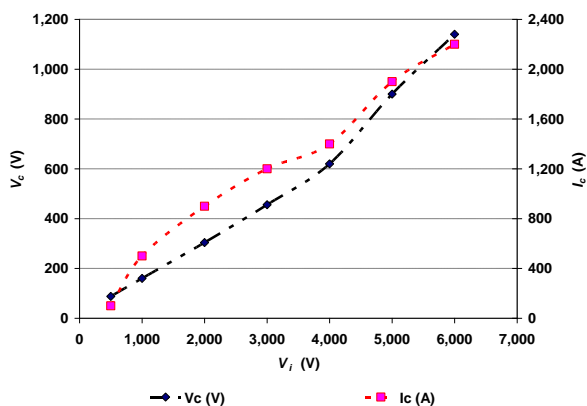


Fig. 8 Curves of V_c - V_i and I_c - V_i of gas tube arrester.

Table 4 Test data of the zener diode.

V_i (V)	V_c (V)	I_c (A)
250	72	50
500	96	85
1,000	160	180

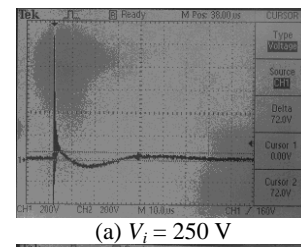
cut voltages and cut currents on the zener diode.

Fig. 9 shows the test data of cut voltage waveforms at impulse voltage (a) 250 V, (b) 500 V and (c) 1 kV, on the zener diode.

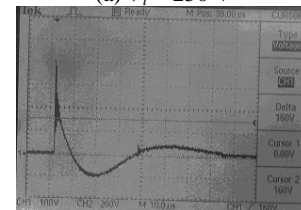
Fig. 10 shows a sample of cut current waveform of test result on the zener diode.

Fig. 11 shows the cut voltage and current curves versus the impulse voltage on the zener diode. Generally, the cut voltages and currents would rise as the impulse voltages increased.

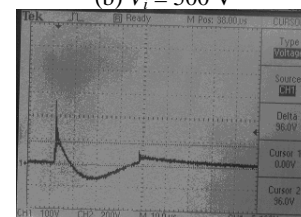
The cut voltage and cut current waveforms were not



(a) $V_i = 250$ V



(b) $V_i = 500$ V



(c) $V_i = 1$ kV

Fig. 9 Cut voltage waveforms of zener diode test results.

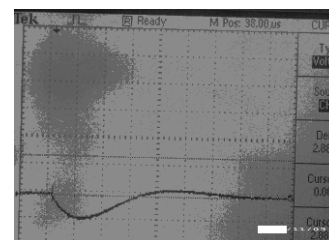


Fig. 10 Cut current waveform of zener diode test result.

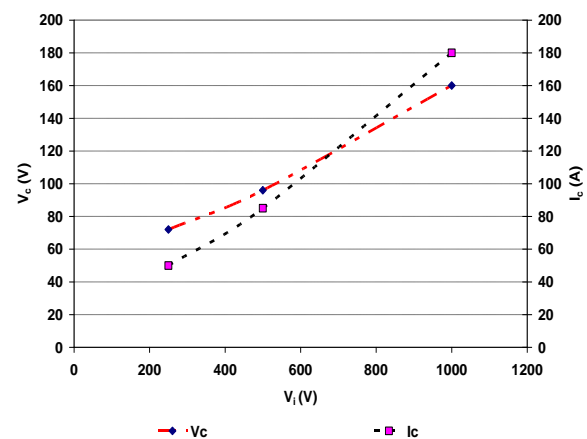


Fig. 11 Curves of V_c - V_i and I_c - V_i for zener diode.

constant and looked more serrature or dense oscillation. This should be reduced by reducing installation cable. The voltage waveforms could also be seen indirectly toward zero. Nevertheless, there was little residue due

to an arc voltage.

The spark gap arrester testing was performed by applying the impulse voltages in ranging of 1-6 kV. The recorded data were the testing data when the spark gap arrester began to breakdown. The obtained data are listed in Table 5. The table lists the values of impulse voltage, cut voltage and cut current.

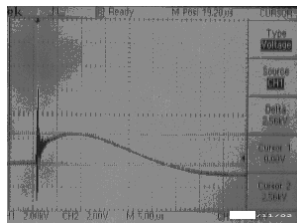
The samples of cut voltage and cut current waveforms are shown in Figs. 12 and 13.

It could be made the cut voltage and the cut current curves versus the impulse voltage of the spark gap arrester. These curves are shown in Fig. 14.

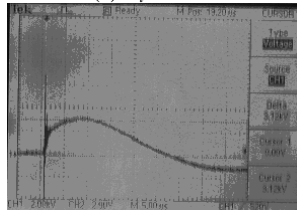
The cut voltage and cut current trends were nearly similar. The voltage waveforms were looked directly

Table 5 Test result data of the spark gap arrester.

V_i (V)	V_c (V)	I_c (A)
1,000	920	0
2,000	1,800	900
3,000	2,320	1,200
4,000	2,560	2,100
5,000	2,930	2,600
6,000	3,120	2,900



(a) $V_i = 4$ kV



(b) $V_i = 6$ kV

Fig. 12 Cut voltage waveforms of spark gap arrester.

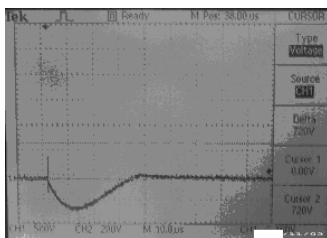


Fig. 13 Cut current waveform of spark gap arrester.

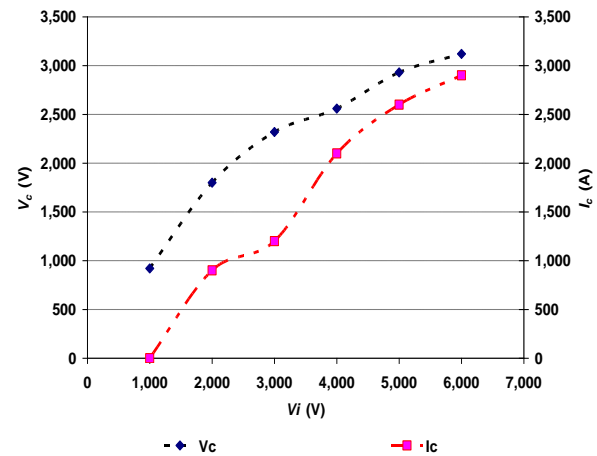


Fig. 14 Curves of V_c - V_i and I_c - V_i of spark gap arrester.

towards zero, but there was little residue in the form of an arc voltage. Some testings showed the voltage and current went beyond to zero and entered to the negative area. This was due to the energy released by an inductive component either in the arrester or generator circuits, after these components stored magnetic energy. The energy was absorbed by the arrester and released in thermal energy arc form.

The varistor arrester testings began in range 565 V-6 kV. Table 6 lists the correlation data between the impulse voltage and the cut voltages and the cut currents of the varistor.

The samples of cut voltage and cut current waveforms of varistor arrester test results are shown in Fig. 15.

Fig. 16 shows a sample of the cut current waveform of the varistor arrester for the impulse voltage of 4 kV.

Fig. 17 shows the curves of cut voltage and cut current versus the impulse voltages for the varistor. The specific behavior of the varistor arrester was seen

Table 6 The varistor arrester testing results.

V_i (V)	V_c (V)	I_c (A)
565	252	20
1,000	348	199
2,000	440	720
3,000	656	1,270
4,000	848	1,790
5,000	1,040	2,340
6,000	1,340	2,900

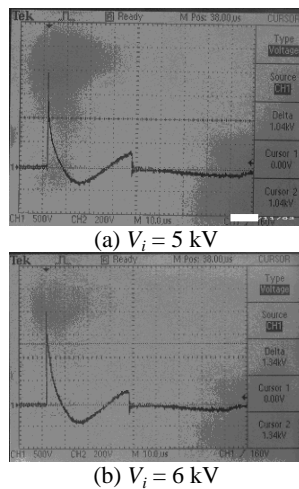


Fig. 15 Cut voltage waveforms of varistor arrester testings.

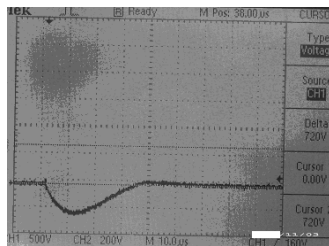


Fig. 16 Cut current waveform of varistor arrester.

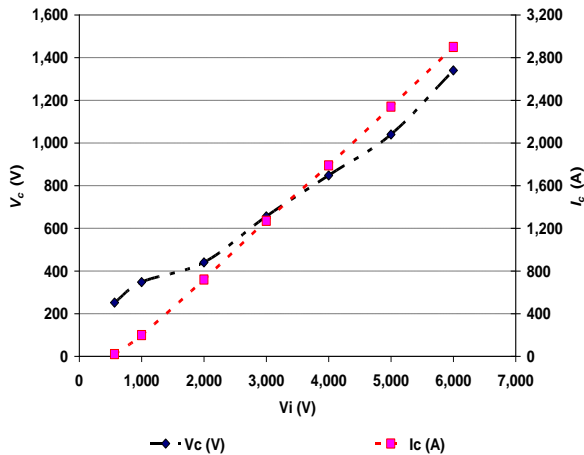


Fig. 17 Curves of V_c - V_i and I_c - V_i for the varistor.

its voltage clamping, before voltage drops to zero, and an undershoot voltage surge occurs. This was caused

by the inductance arrester parameters, testing circuit or generator inductance which releases the current after the cut voltage toward zero.

The testings with the decoupling coils were to get voltage drops and time delay, used the elements of iron, air and ferrite cores, which yielded data as listed in Table 7 [45].

The decoupling coils are shown in Fig. 18.

The impedance of the ferrite core decoupling element had the highest value among remaining cores. This case caused a voltage drop as the product of impedance and the current passing through element. It could create the spark gap arrester work faster than the remaining cores. The impedance of iron core decoupling element was different from the air core one due to the hysteresis and eddy current losses was taking part to the change. It was useful for determining the voltage drop of decoupling element in the design of arrester protection cascade coordination. A concern thing was an element impedance change existence as function of current, so that the determination of R , L , and C were not enough to determine the impedances.

The test results of cascade arresters were in the forms of cut voltages. The ferrite core decoupling element was the fastest to arrester work. It could be proved by the test cascade, that the arrester spark gap was always faster to work using ferrite core decoupling element, due to the higher voltage drop was summed the cut voltage of the varistor. Fig. 19 shows the cascade arrester voltage and current waveforms on the air core decoupling element.

Fig. 20 shows the cascade arrester voltage and current waveforms on the iron core decoupling element.

Table 7 The decoupling element parameter values.

Turns	Ferrite core				Air core				Iron core			
	R (Ω)	L (μ H)	C (μ F)	Z (Ω)	R (Ω)	L (μ H)	C (μ F)	Z (Ω)	R (Ω)	L (μ H)	C (μ F)	Z (Ω)
42	0.043	133.6	8.0	0.601	0.02	2.2	27.99	0.0343	0.054	14.7	38.60	0.211
82	0.076	273	4.6	4.354	0.046	27.6	8.83	0.363	0.416	129	11.45	2.174

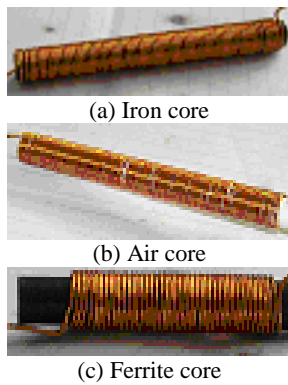


Fig. 18 The iron, air and ferrite decoupling coil cores.

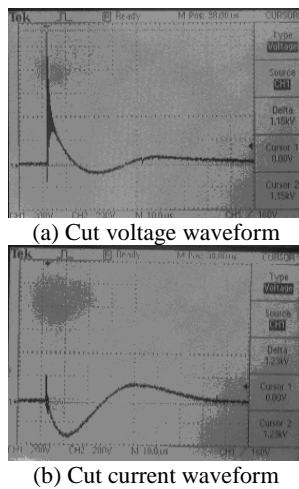


Fig. 19 Cascade arrester waveforms of air core element.

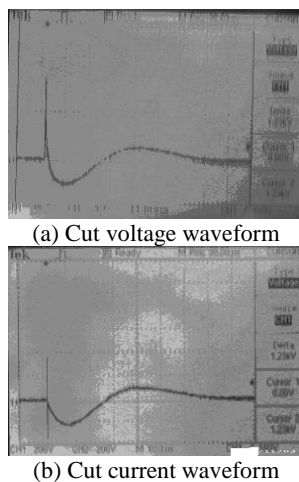


Fig. 20 Cascade arrester waveforms of iron core element.

Fig. 21 shows the cascade arrester voltage and current waveforms on the ferrite core decoupling element.

The value of initial breakdown voltage of the spark gap changed due to the cascade circuit existence. To create a spark gap arrester breakdown, it was required

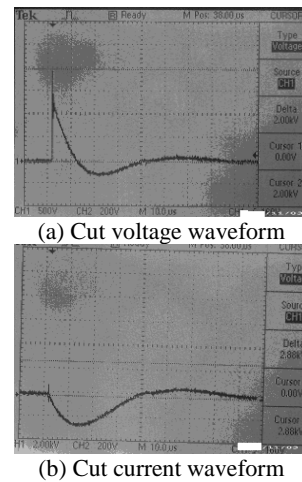


Fig. 21 Cascade arrester waveforms of ferrite core element.

a higher voltage. This case was caused by change in the voltage waveform became a cut voltage waveform because of the varistor. The voltages subjected to the spark gap were decoupling element voltage drops summed to the varistor cut voltages.

Before the spark gap arresters worked, the entire current passed through the varistor and decoupling elements. This current was a reference of varistor work planning. After it worked, the varistor was traversed by the current of 0.32 up to 10% only. Thus, it was to be noted how much capacity of the spark gap arrester was required, depending on the current through the system planning of lightning protection. While, the cut voltage of varistor arrester in the cascade circuit, tends to be relatively constant.

For choice of decoupling element core, it could be determined through a arrester cascade cut voltage, with various core kinds. By the change of impulse voltage sharpness, it would show the cut voltage with a high enough frequency on the air core decoupling element, that was about 400 kHz, it was about 100 kHz on the ferrite core decoupling element, and it did not arise an oscillation on the iron core decoupling element. If the system protected working with frequency range several hundred kilohertz, the iron core decoupling element was the best choice.

It was found an undershoot voltage waveform in the varistor. This case could be a serious problem if it

increased and reached a value equal to the input impulse voltage. Therefore, it was necessary to increase the decoupling element impedance up to the element drop voltages which were high enough to make the spark gap arrester work.

4. Conclusions

It could be seen that the steady state output voltages tend to be linear. The arresters did not disturb the system line voltages. Otherwise, based on the impulse tests the varistor and gas tube arresters had almost the same initial cut voltages, whereas the highest cut voltage was occurred on the spark gap, as around 1 kV. For the oscillation wave phenomena, the gas tube and varistor arresters had at least oscillation compared to the zener diode and spark gap arresters.

The change of decoupling element cores in the arrester cascade would make the resistance, inductance and capacitance changed significantly. The decoupling element impedance of the ferrite core was the highest, followed by the iron and air cores ones respectively. Thus, the coordination of arrester cascade decoupling element with the ferrite core would work fastest compared to the remaining cores in the same impulse value.

Acknowledgments

Authors here with respect offer thanks to High Voltage and High Current Laboratory STEI-ITB and National Institute of Technology (Itenas) Bandung for supporting the research project and publication.

References

- [1] Cooray, V. 2010. *Lightning Protection, The Institution of Engineering and Technology*. IET Power and Energy Series 58.
- [2] Seraudie, C. 1999. LV Surges and Surge Arresters, LV Insulation Co-ordination, Cahier Technique No. 179, Schneider Electric.
- [3] Cohen, R. L. 2005. *How to Protect Your House and Its Contents From Lightning: Surge Protection, IEEE Guide for Surge Protection of Equipment Connected to AC Power and Communication Circuits*. Standards Information Network, IEEE Press.
- [4] Pryor, L. 2016. "The Application and Selection of Lightning Arresters." Accessed March 6, 2016. apps.geindustrial.com.
- [5] Ali, S. A. 2013. "Design of Lightning Arresters for Electrical Power Systems Protection." *Power Engineering and Electrical Engineering* 11 (6): 433-42.
- [6] Dehn. 2012. *Lightning Protection Guide*, Revised 2nd edition, Germany: 14-6.
- [7] Mata, C. T., Rakov, V. A., Rambo, K. J., Diaz, P., Rey, R., and Uman, M. A. 2003. "Measurement of the Division of Lightning Return Stroke Current among the Multiple Arresters and Grounds of a Power Distribution Line." *IEEE Transactions on Power Delivery* 18 (4): 1203-8.
- [8] Stallinsa, J. A., and Bentley, M. L. 2006. "Urban Lightning Climatology and GIS: An Analytical Framework from the Case Study of Atlanta." *Applied Geography* 26 (3-4): 242-59.
- [9] Naccarato, K. P., Pinto, J. O., and Pinto, I. R. C. A. 2003. "Evidence of Thermal and Aerosol Effects on the Cloud-to-Ground Lightning Density and Polarity over Large Urban Areas of Southeastern Brazil." *Geophysical Research Letters* 30 (13): 71-4. doi:10.1029/2003GL017496.
- [10] Soriano, L. R., and Pablo, F. 2002. "Effect of Small Urban Areas in Central Spain on the Enhancement of Cloud-to-Ground Lightning Activity." *Atmospheric Environment* 36 (17): 2809-16.
- [11] Pinto, I. R. C. A., Pinto, J. O., Gomes, M. A. S. S., and Ferreira, N. J. 2004. "Urban Effect on the Characteristics of Cloud-to-Ground Lightning over Belo Horizonte-Brazil." *Annales Geophysicae* 22 (January): 697-700.
- [12] Lowke, J. J., Smith, D., Nelson, K. E., Crompton, R. W., and Murphy, A. B. 2012. "Birth of Ball Lightning." *Journal of Geophysical Research* 117 (October): 1-7.
- [13] Podporkin, G. V., Pilshikov, V. E., and Sivaev, A. D. 2016. "Application of Long Flashover Arresters for Improvement of Lightning Protection and Operating Voltage Reliability of Distribution Lines." Appalachian State University. Accessed March 6, 2016. <http://www.appstate.edu/~clementsjs/surfaceflashover/lightningflashover.pdf>.
- [14] Vladimir, G. 2007. "High Current Pulse Transducer for Metal-Oxide Surge Arresters." *UDC* (2): 22-4.
- [15] Chiesa, N. 2010. "Power Transformer Modeling for Inrush Current Calculation." Ph.D. thesis, Norwegian University of Science and Technology.
- [16] Milardic, V., Uglesic I., and Pavic, I. 2008. "Selection of Surge Protective Devices for Low-Voltage Systems Connected to Overhead Line." *IEEE Transactions on Power Delivery* 25 (3): 1530-7.
- [17] Dau, S. K. O. 2008. "Modelling of Lightning Overvoltages for the Protection of Transmission Lines by

- Means of Shielding Wires and Surge Arresters.” Ph.D. Thesis, AGH University of Science and Technology.
- [18] Chai, Y. J., Zhou, W. J., He, R. D., and Zhao, L. X. 2007. “Experimental Study on Lightning Characteristics of Electronic Equipment’s Power Supply.” In *Proceedings of the World Congress on Engineering*, 1-4.
- [19] Eaton. 2015. Storm Trapper High Energy Low-Voltage Distribution-Class MOV Surge Arrester, Surge Arresters Catalog Data CA235015EN (April).
- [20] Paul, D. 2001. “Low Voltage Power System Surge Overvoltage Protection.” *IEEE Transactions on Industry Applications* 37 (1): 223-9.
- [21] Ardley, T. 2008. *First Principles of a Gas Discharge Tube (GDT) Primary Protector*. Bourns, Inc.
- [22] Piantini, A. 2008. “Lightning Protection of Overhead Power Distribution Lines.” Presented at the 29th International Conference on Lightning Protection, Uppsala, Sweden.
- [23] Sanabria, D. R., and Robles, C. R. 2003. “Lightning and Lightning Arrester Simulation in Electrical Power Distribution Systems.” University of Puerto Rico Mayagüez. Accessed March 6, 2016. http://ece.uprm.edu/~lorama/Proy_Rayos03.pdf.
- [24] Chrzan, K. L. 2004. “Influence of Moisture and Partial Discharges on the Degradation of High-Voltage Surge Arresters.” *European Transactions on Electrical Power* 14 (3): 175-84.
- [25] Strmika, R. 2003. “Lightning Arresters’ effect on Power Line Reliability.” In *Proceedings of the 2003 InfraMation Conference*, 1-5.
- [26] Hasse, P. 2000. *Overvoltage Protection of Low Overvoltage Systems*. 2nd edition, London: The Institution of Engineering and Technology.
- [27] Woodworth, J. 2008. *Guide For Selecting an Arrester Field Test Method*. ArresterWorks.
- [28] Meppelink, J., Drilling, C., Droidner, M., Jordan, E. G., and Trinkwald, J. 2016. “Lightning Arresters with Spark Gaps, Requirements and Future Trends of Development and Applications.” Accessed March 6, 2016. <http://obo.at/downloads/FUNKENS2.PDF>.
- [29] EPCOS. 2015. *Surge Arresters and Switching Spark Gaps*. Munich: EPCOS Product Profile.
- [30] Bouqueneau, C. 2006. “The Lightning Protection International Standard.” In *Proceedings of the 28th International Conference on Lightning Protection*, 1-6.
- [31] Hill, K. 2004. *Surge Arresters and Testing*. Double Engineering Company, 1.
- [32] Thipprasert, W., and Sritakaew, P. 2014. “Leakage Currents of Zinc Oxide Surge Arresters in 22 kV Distribution System Using Thermal Image Camera.” *Journal of Power and Energy Engineering* 2 (4): 712-7.
- [33] Hosseini, S. A., Razavi, F., Karami, M., Ghadimi A. A., and Madahi, S. S. K. 2012. “A New Method to Recognize the Status of SiC Surge Arresters in Substations.” *Indian Journal of Science and Technology* 5 (5): 2692-700.
- [34] Eaton. 2009. *Eaton’s Guide to Surge Suppression—Applications Notes*. Eaton Corporation Eaton’s guide to surge suppression.
- [35] FLPA (French Lightning Protection Association). 2000. *Precautions to be Considered for Use of Surge Arresters Tested According to Class 1 of IEC 61643-1*. French Lightning Protection Association.
- [36] Díaz, R., Fernández, F., and Silva, J. 2001. “Simulation and Tests on Surge Arresters in High-Voltage Laboratory.” Universidad Nacional de Tucumán. Accessed March 6, 2016. <http://www.herrera.unt.edu.ar/alta-tension/lat/publicaciones/paper2vf.pdf>.
- [37] Darus, A. B., Malek, Z. A., Afendi, M., and Piah, M. 2004. “New Design of High Voltage Surge Arresters.” Universiti Teknologi Malaysia. Accessed March 6, 2016. http://www.energy.siemens.com/hq/pool/hq/power-transmission/high-voltage-products/surge-arresters-and-limiters/Catalogue_HV_surge_arresters_en.pdf.
- [38] Mardira, K. P., and Saha, T. K. 2002. “Modern Electrical Diagnostics for Metal Oxide Surge Arresters.” *Transmission and Distribution Conference and Exhibition* 2 (October): 672-6.
- [39] Michalopoulos, A. 2011. *Consideration of Surge Arresters for Low Voltage Mains Applications*. Master of Science in Engineering, Johannesburg.
- [40] WG A3.17, 2016. *Evaluation of Stresses of Surge Arresters and Appropriate Test Procedures, International Council on Large Electric Systems*. Working Group A3.17, Cigre. <http://www.cigre.org>.
- [41] W.G.C4.408. 2013. *Lightning Protection of Low-Voltage Networks*. Paris: Cigre.
- [42] Kanashiro, A. G., Zanotti, J. M., Obase, P. F., and Wilson, R. B. 2009. “Diagnostic of Silicon Carbide Surge Arresters of Substation.” *Wseas Transactions on Systems* 8 (12): 1284-93.
- [43] Richer, B., Schmidt W., Kannus, K., Lahti, K., Hinrichsen, V., Neumann, C., Petrusch W., and Steinfeld, K. 2004. “Long Term Performance of Polymer Housed MO Surge Arresters.” *CIGRÉ A3-110*: 1-8.
- [44] Asaadi, J., Conrad, J. M., Gollapinni, S., Jones, B. J. P., Jostlein, H., John, J. M. S., Strauss, T. S., Wolbers, S., and Zennamo, J. 2014. “Testing of High Voltage Surge Protection Devices for Use in Liquid Argon TPC Detectors.” *Journal of Instrumentation* 9 (September): 1-22.
- [45] Waluyo, and Hutasoit, Y. M. 2011. “The Influences of Decoupling Elements on the Testing of Low Voltage Spark Gap and Varistor.” In *Proceedings of the 46th International Universities Power Engineering Conference*, 1-5.